Photophysics of conjugated polymers: the contribution of ultrafast spectroscopy

2002 J. Phys.: Condens. Matter 14 9785

(http://iopscience.iop.org/0953-8984/14/42/301)

INSTITUTE OF PHYSICS PUBLISHING JOURNAL OF PHYSICS: CONDENSED MATTER

J. Phys.: Condens. Matter **14** (2002) 9785–9802 PII: S0953-8984(02)37129-7

Photophysics of conjugated polymers: the contribution of ultrafast spectroscopy

Christoph Gadermaier[1,2,3] **and Guglielmo Lanzani**[3]

[1] Christian Doppler Laboratory of Advanced Functional Materials, Institute of Solid State Physics, Graz University of Technology, Petersgasse 16, 8010 Graz, Austria
[2] Christian Doppler Laboratory of Advanced Functional Materials, Institute of Nanostructured Materials and Photonics, Franz-Pichler-Str. 30, 8160 Weiz, Austria
[3] Dipartimento di Fisica, Politecnico di Milano, Pzza L da Vinci 32, 20133 Milano, Italy

Received 17 May 2002
Published 11 October 2002
Online at stacks.iop.org/JPhysCM/14/9785

Abstract

This article attempts to present a comprehensive picture of the elementary processes in conjugated polymers. Key experiments using ultrafast techniques are described, which provide insights into excitation energy migration in homopolymers as well as guest–host systems, charge-carrier generation both intrinsic and in donor–acceptor systems, and the various mechanisms leading to triplet states.

1. Introduction

Conjugated organic materials are currently experiencing the dawn of their commercialization in electroluminescent and photovoltaic devices. Recently, an electrically pumped laser has been realized by using an organic conjugated molecular single crystal [1]. The physics of conjugated systems has been under investigation since the early days of quantum mechanics and the understanding of fundamental properties has consistently underpinned the achievements in practical applications. At this point a rather comprehensive background for discussing the optical and electrical properties has been established; however, some critical issues are still unclear. This article attempts to remedy this by presenting an overall picture, drawn from the insights gained via time-resolved spectroscopy, which is a powerful tool for investigating elementary excitation dynamics, and has contributed significantly to this field, in particular by enhancing the understanding of the fundamental photophysics.

Initially, conjugated polymers (CPs) were described as one-dimensional semiconductors, which led to the development of the Su–Schrieffer–Heeger model [2], backed by the early results on *trans*-polyacetylene (*trans*-PA). Within this model the elementary excitations of CPs are self-trapped electrons and holes, energetically split off the valence and conduction bands into the gap. The limitations of this description are rooted in the neglect of coulombic electron–hole interaction as well as the particularity of *trans*-PA, which is distinguished from other CPs by its degenerate electronic ground state, and hence displays its own zoo of photoexcited

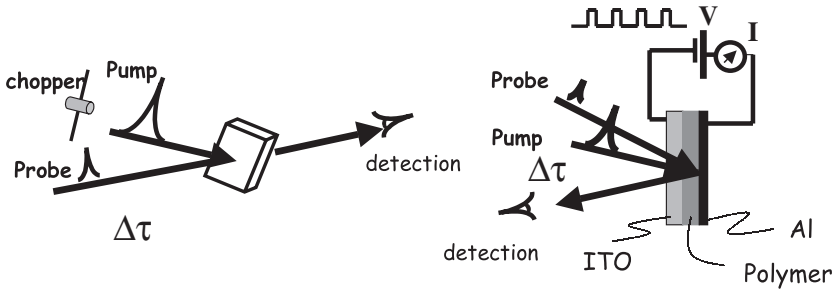

Figure 1. Schematic diagrams of the pump–probe and field-induced pump–probe set-ups.

species. Moreover, infinitely long chains are assumed, while effective conjugation lengths achieved in practice rarely exceed 50 carbon atoms.

An alternative approach to achieving an understanding of the physics of CPs is founded on the molecular nature of these materials. It describes the disordered polymer bulk as an array of conjugated segments with molecular-like properties (fluorophores, if the emphasis is on their luminescent properties) [3], originating from subunits of the polymer chain separated by topological faults. The broad absorption spectra of CPs are explained in terms of inhomogeneous linewidths arising from variations in length and environment of the conjugated segments. In this picture, which is adopted in the present work, the elementary electronic excitations are singlets (S_n), triplets (T_n) and radical ion (doublet D_n—also called polaron) states. The strong coupling of the optical transitions to certain molecular vibrations (Franck–Condon modes) gives rise to sidebands in the optical spectra (vibronic progressions or satellites). Following photoexcitation, the vibrational energy initially stored in a few optically coupled modes is very quickly ($\sim$100 fs) redistributed over non-coupled modes (these are not directly visible in optical experiments; sometimes they are referred to as dark modes), which indicates a large anharmonicity of the nuclear potential. In small organic molecules, dark vibrational modes are known to live for several picoseconds, while no direct measurements have been made so far on long conjugated chains. It is conjectured that such dark vibrational energy acts as a reservoir for charge separation via thermally activated tunnelling—see below.

Solid-state effects are weak perturbations of the intrachain dynamics leading to spectral broadening, energy migration and charge separation as a consequence of intermolecular coupling. 'Weak' intermolecular coupling does not mean 'negligible'; on the contrary, effects on the kinetics and decay paths can be dramatic. For instance, the PL quantum yield is drastically reduced when the chains are in solution, due to non-radiative paths that open up in the solid state.

2. The pump–probe experiment

Excited state transmission spectra can be measured by pump–probe experiments, in which two optical pulses reach the sample (see figure 1). The pump pulse resonantly excites the sample; the probe pulse, time delayed and weaker, is used to measure induced transmission changes (assuming negligible probe perturbation). It is a two-photon process, third order in the wave interaction picture (i.e. depending on χ^3). The simplest description is however based on the *effective* first-order response function from the excited state, as follows. The pump pulse induces population redistribution among the electronic levels of the excited sample. If $N_k(t)$ is the population of the k-level during and after the pump, the probe transmission associated

with $k \rightarrow j$ electronic transitions is the correlation function:

$$T^*(\omega, \tau) = \frac{\int \mathrm{d}t\, I_{pr}(\omega, t-\tau) \exp\left[-\sum_{kj} \sigma_{kj}(\omega) N_k(t) D\right]}{\int \mathrm{d}t\, I_{pr}(\omega, t)} \tag{1}$$

where τ is the pump–probe delay, $I_{pr}(\omega, t)$ is the probe pulse intensity at frequency ω, $\sigma_{kj}(\omega)$ is the transition cross-section that contains the spectral line shape and D is the sample thickness. The experimental observable is the change of the optical density, or absorbance:

$$\Delta\mathrm{OD} = -\ln\left(\frac{T^*}{T}\right) = -\ln\left(1 + \frac{\Delta T}{T}\right) \cong -\frac{\Delta T}{T} \tag{2}$$

where T^* (T) is the transmission in the excited (unexcited) sample and the last approximation is valid for small signals (<10%).

If the impulsive approximation holds true, i.e. when the pump pulse duration is much shorter than the kinetic process under study, the previous equations become simpler:

$$\begin{aligned}\Delta\mathrm{OD} &= -\ln\left(\frac{\exp\left[-\sum \sigma_{kj}(\omega) N_k(t) D\right]}{\exp\left[-\sum \sigma_{kj}(\omega) N_k D\right]}\right) = -\ln\left(\exp\left[-\sum \sigma_{kj}(\omega)\, \Delta N_k(t)\, D\right]\right) \\ &\approx \sum \sigma_{kj}(\omega)\, \Delta N_k(t)\, D \end{aligned} \tag{3}$$

where $\Delta N_k(t) = N_k(t) - N_k$ is the pump-induced change of the k-state population. With this approximation, the measured quantity is

$$-\frac{\Delta T}{T} = \sum \sigma_{kj}(\omega)\, \Delta N_k(t)\, D \tag{4}$$

which has a *straightforward interpretation*[4]. $\Delta N_0(t)$ accounts for the change in the ground state population N_0, while in general the unexcited populations are $N_k = 0$ for $k \neq 0$.

The transmission difference spectrum, $\Delta T/T(\omega)$, contains only three types of signal: photobleaching (PB), stimulated emission (SE) and photoinduced absorption (PA). PB is the reduction of the optical density in the region of ground state absorption ($\Delta T > 0$). It results from two contributions: depletion of the ground state ($\Delta N_0(t)$) and filling up of the final state (causing SE at the optical gap); its spectral shape resembles that of ground state absorption. SE ($\Delta T > 0$) is the process of light amplification (gain) due to transitions from the occupied states to empty vibronic states. Its spectral shape resembles that of the PL, with some exceptions:

(i) the 0–0 transition merges into PB;
(ii) SE may originate from high vibrational levels of the excited state and be blue-shifted with respect to the PL (hot emission);
(iii) there is a correction factor ω^3 (accounted for by the Einstein theory of spontaneous and stimulated transitions).

Finally, PA is associated with negative ΔT and it is due to optical transitions from the newly occupied states (following photoexcitation) to higher-lying levels.

From the experimental point of view, a $\Delta T/T$ signal is obtained by recording pump–probe events at fixed delay, the number per unit time being limited by the laser repetition rate. Data collection is achieved by phase-sensitive techniques for high enough repetition rates, or using direct pulse storage with a boxcar electronics. Time intervals between pump and probe are set by controlling the optical paths of the two beams. A white-light continuum is used to probe transmission changes over a broad spectral range [4]. Two different sorts of measurement

[4] If the impulsive approximation does not hold, but that of small signal is still valid, the transmission difference is given by $-\Delta T/T = \{\int \mathrm{d}t\, I_{pr}(t-\tau)[\sum_{kj} \sigma_{kj}(\omega) N_k(t) D]\}/\{\int \mathrm{d}t\, I_{pr}(t)\}$.

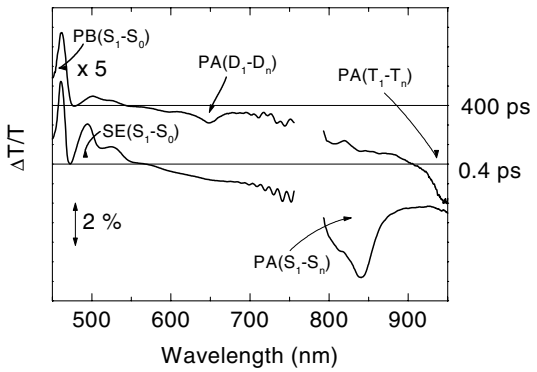

Figure 2. The $\Delta T/T$ spectrum for m-LPPP at different pump–probe delays.

are typically performed: single-wavelength pump–probe delay scans, by spectral selection at the detector entrance; full-spectra acquisition, at fixed pump–probe delay. A good review of time-resolved spectroscopic methods, including technical aspects, and pulse generation, is given in [5]. The workhorse source nowadays almost universally adopted is based on the mode-locked Ti:sapphire laser, often amplified at a 1 kHz repetition rate. Typical parameters are 200 fs pulse duration at 800 nm with nJ to hundreds of μJ of energy per pulse. White light covers the visible range and near-infrared. Parametric conversion is used for tuning the pulse wavelength to the UV and IR [6].

3. Nature of the primary photoexcited states

The typical oscillator strength of the optical transition in a CP is $f = 1$, corresponding, via the approximate Strickler–Berg relation, roughly to a radiative time $\tau = (\frac{\tilde{\nu}^2 f}{1.5})^{-1} = 6$ ns, for a typical emission centre wavenumber in the visible. Due to there being several non-radiative decay paths, the typical lifetime of the singlet state is 0.1–1 ns, which renders transient spectroscopy an important tool for their study. It took several years to reach a broadly agreed assignment of the transient spectra, with some doubts still remaining. One major problem is the vast number of different materials existing in which small chemical or morphological variations as well as contamination may induce substantial modification of the properties. This has certainly influenced the evolution of the picture of ultrafast photophysics in CPs, which initially concentrated on the (para)-phenylene vinylene (PPV) family.

As a case study, however, it is instructive to start with m-LPPP, a poly(para-phenylene) backbone incorporated into a ladder-type molecular structure to increase intrachain order and reduce defect content. A comparatively high PLQY of 30% is observed in bulk films [7]. LEDs [8] and optically pumped lasers [9, 10] have been demonstrated.

In TA experiments, m-LPPP shows a particularly high SE [11], since the gain region does not overlap with the PA, at least at medium excitation density, which is a necessary condition for the possible use in solid-state lasers. The transient spectra and their assignments to the elementary photoexcitations for m-LPPP are shown in figure 2.

The ubiquitous overlap of SE and PA related to charged states have caused substantial confusion in the previous assignment, out of which interesting concepts such as polaron pairs, i.e. a pair of coulombically bound opposite charges, possibly on different chains, have emerged.

TA experiments on pristine and photo-oxidized PPV films [12] showed that in pure film the primary photoexcitations are in the singlet, whereas fast charge separation from singlets,

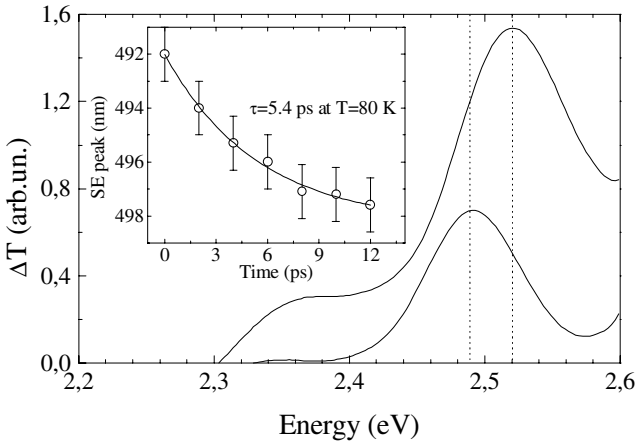

Figure 3. The transient red-shift of the SE in *m*-LPPP.

possibly on photogenerated carbonyl groups, can be assumed in the photo-oxidized samples. The SE of these samples overlaps with PA, the latter being dominant in the photo-oxidized samples, where it shows a decay component that follows SE plus a slower one which can be attributed to the charge-separated species [13]. The earlier conjecture of initial branching between neutral and charged states was probably invoked to account for measurements made on samples that were unintentionally photo-oxidized during the experiment.

Besides the spectral overlap problem, the transient behaviour of the singlet PA is often different from the time traces obtained from time-resolved fluorescence measurements. This discrepancy has been resolved by Maniloff *et al* [14], who studied a variety of PPV samples and found that both types of dynamics depend on the excitation density n_{exc} and that they match when they are measured at the same n_{exc}. This dependence can be explained by bimolecular annihilation of S_1 states, due to a transfer of excitation energy from one excited conjugated unit to another, which leaves one in the ground state:

$$S_1 + S_1 \rightarrow S_n + S_0. \tag{5}$$

The fate of S_n will be discussed below in more detail; as a first approximation it can be assumed that it rapidly relaxes towards S_1. The temporal evolution of the S_1 population can therefore be described by the rate equation

$$\frac{dS_1}{dt} = -\beta S_1 - \gamma(t) S_1^2 \tag{6}$$

where $\gamma(t)$ is constant in the strong-diffusion limit, while it is proportional to $t^{-1/2}$ in the diffusion-free limit [15]. Since this intensity dependence has not been found for chains in solution, it can be assumed that the annihilation process is efficient only between polymer chains in close proximity, not between conjugated segments on the same chain, which have a low transition dipole interaction.

The red-shifts between time-integrated PL and absorption spectra are caused by the energy relaxation of the photoexcitations within the inhomogeneously broadened density of states (DOS) distribution. Evidence for this excitation energy migration (EEM) is given by the transient red-shift of the spectral features and the loss of pump-induced dichroism. The SE in *m*-LPPP has been found to undergo a fast transient red-shift by about 30 meV (figure 3) within a few picoseconds [16], which is also the timescale of the polarization memory loss.

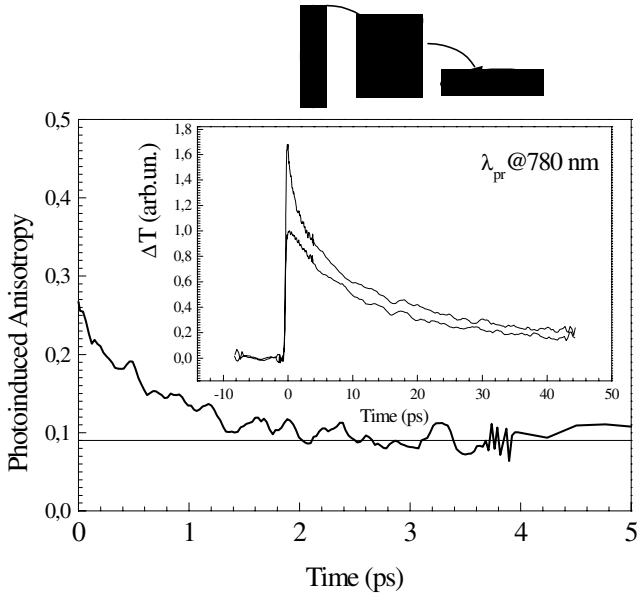

Figure 4. The anisotropy $f(t)$ (see the text) of the S_1 absorption in *m*-LPPP. The inset shows the components with polarization parallel and perpendicular to the pump pulse.

This confirms the assumption that the S_1 state migrates across the conjugated units of the disordered bulk film, preferentially to units of lower transition energy. These results from TA experiments enabled the determination of the characteristic time for EEM. Measuring the polarization $f(t)$ in ΔT under identical experimental conditions, we can work out the actual time constant of the migration process in our devices:

$$f(t) = \frac{(\Delta T/T)_{par} - (\Delta T/T)_{perp}}{(\Delta T/T)_{par} + 2(\Delta T/T)_{perp}} \tag{7}$$

with the subscripts par and $perp$ indicating the differential transmission for pump and probe with parallel and perpendicular polarizations with respect to each other. The result is plotted in figure 4.

4. Photogeneration of charge carriers

As mentioned above, upon optical excitation of CPs from the electronic ground state, in addition to the singlet, frequently one also encounters charged states [17]. Assuming that their absorption cross-section is comparable to that of the singlet, from transient spectra it can be deduced that the efficiency of charge photogeneration (CPG) ranges from 1 to 10% (in donor–acceptor systems it can be as high as 100%).

As a result of the distribution of site energies with varying spatial distances as well as energetic alignment of the HOMO and LUMO levels between adjacent sites, the probability of exciton dissociation can vary strongly between different sites. Therefore CPG is mediated by migration of the S_1 states, which visit a number of sites and are likely to encounter one with a high dissociation probability.

One way to study the dynamics of CPG is to modulate its efficiency, e.g. by enhancing the S_1 dissociation by the application of an electric field or by exciting S_1 to a higher state S_n. The

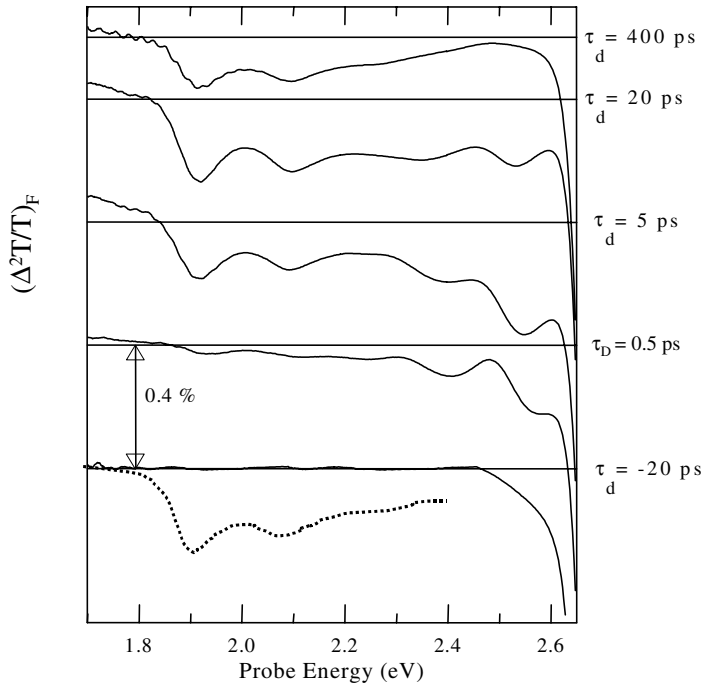

Figure 5. The field-induced $\Delta T/T$ spectrum of *m*-LPPP (from [17]).

first studies of this type relied on indirect evidence such as PL quenching due to dissociation of the emitting S_1 states. For a PPV film blended into polycarbonate, Kersting *et al* [18] found that the field-induced PL quenching shows a temporal evolution similar to that of the EEM. The significance of the migration was confirmed by later findings of the same group, such as the excitation energy dependence of the photocurrent (PC)—the PC action spectrum—which does not follow the ground state absorption spectrum: higher excitation energy creates an S_1 population with a higher mean energy and hence a longer mean migration length [19].

Field-induced changes in $\Delta T/T$ are measured by modulating the electric field and referencing the lock-in amplifier to this modulation; a sketch of the experiment is given in figure 1. Since it is a variation of $\Delta T/T$, this signal will be referred to as $(\Delta^2 T/T)_F$. As depicted for *m*-LPPP in figure 5, $(\Delta^2 T/T)_F$ has the opposite sign to $\Delta T/T$ for the singlet features and the same sign for the polaron PA, which is direct evidence for the enhancement of charges at the expense of singlets [20].

Information on the kinetics of the field-induced singlet breaking process are extracted by time traces of the $(\Delta^2 T/T)_F$ signal at selected probe energies. Figure 6 depicts these time traces at the singlet SE (2.53 eV) and at its PA_1 (1.51 eV), together with the polaron feature PA_2 (1.91 eV). The field-induced polaron absorption has an initial fast rise, growing to ≈50% of its final value in 2 ps (figure 6(a)); this is followed by a slower increase on the 40 ps timescale (figure 3(b)) and a plateau on the 400 ps timescale (figure 6(c)). The field-induced SE and PA_1 quenching also show an initial fast rise, reaching their maximum values by $\tau_D = 2$ ps, followed by a slow decay; for longer time delays the signals vanish due to recombination. Note that the dynamics of the $(\Delta^2 T/T)_F$ signals is completely different from that of the corresponding $\Delta T/T$ signals. The interpretation of these data is complicated by the presence of comparatively fast radiative and non-radiative decay channels for the singlet, which compete with the field-induced dissociation.

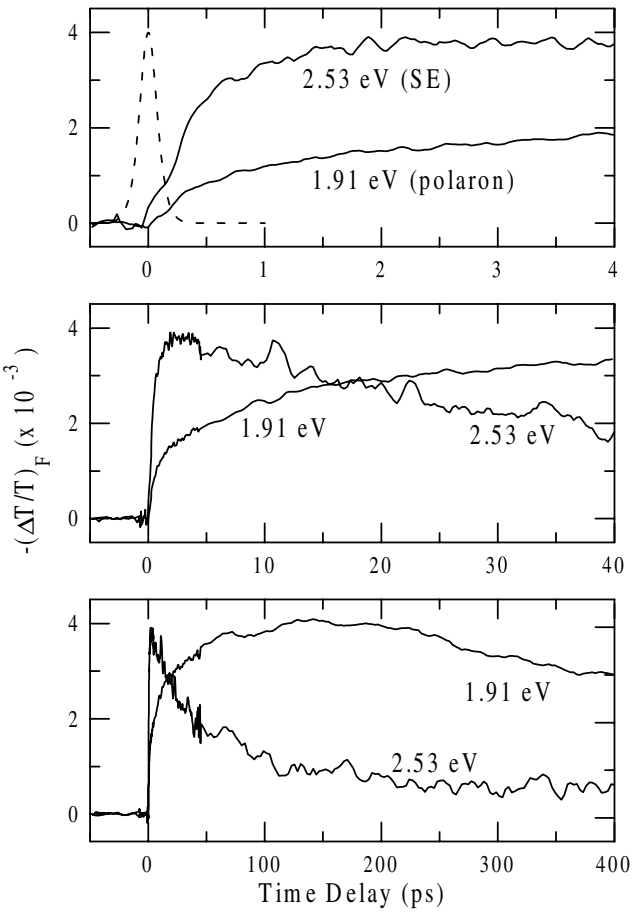

Figure 6. Field-induced $\Delta T/T$ time traces of *m*-LPPP (from [17]).

In order to untangle the field-induced charge generation from the singlet exciton decay dynamics, one can define the following phenomenological time-dependent parameter, which represents the field-induced singlet breaking rate:

$$\gamma(t) = \frac{1}{N_{SF}} \frac{\mathrm{d}N_{PMF}}{\mathrm{d}t} = \frac{\sigma_S}{\sigma_P} \frac{1}{\mathrm{SE}_F} \frac{\mathrm{dPA}_{MF}}{\mathrm{d}t} \tag{8}$$

where $N_{SF} = \mathrm{SE}_F/\sigma_S$ is the change in the singlet exciton population in the presence of electric field, $N_{PMF} = \mathrm{PA}_{MF}/\sigma_P$ is the field-induced polaron population, σ_S (σ_P) is the cross-section for SE (polaron absorption).

The plot of $\gamma(t)$, shown in figure 7, suggests that CPG occurs in two separate time regimes. One mechanism is highly dispersive and takes place within the first 2–3 ps. The other is only weakly time dependent and persists for longer delays. The initial time dependence closely resembles that of migration (compare with figures 3 and 4). The lack of electric field dependence of the CPG kinetics can be considered as further evidence of the diffusion-limited nature of the proposed dissociation process. Within this model, CPG becomes negligible once the excitons have reached the bottom of the DOS, where their mobility is drastically reduced [21]. The small and weakly time-dependent CPG that persists at longer delays is a joint effect of residual migration and dissociation from less favourable sites.

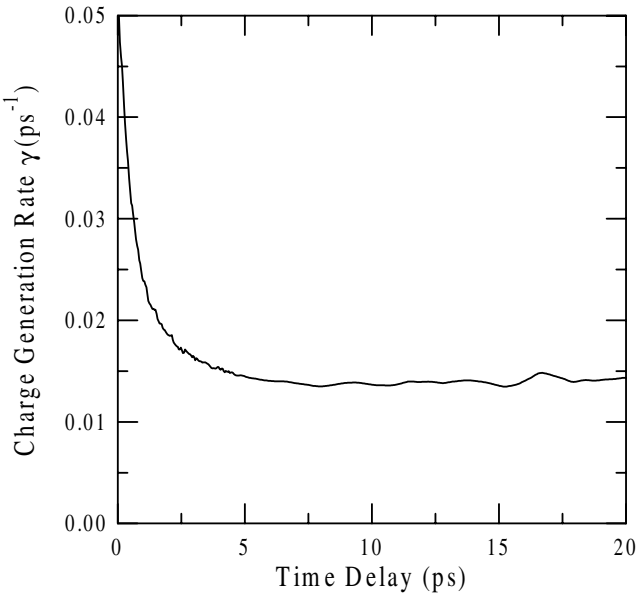

Figure 7. Temporal behaviour of the field-induced exciton breaking rate.

As mentioned above, to a certain extent migration can also explain the increase of the CPG efficiency with higher excitation energy, but not up to 1.5 eV above the absorption edge, as has been found in *m*-LPPP [22]. This behaviour can only be rationalized if the singlet dissociation probability $p_k(i)$ of a state k at site i (i is intended as an index running over the sites) is a function of the excitation energy E_{exc}. There are at least two possible mechanisms that lead to such dependence.

Initially, the excess energy is stored in a small number of vibrational modes that are optically coupled to the electronic transition. In optical experiments this vibrational energy appears to be dissipated within 100 fs via two mechanisms: *on-site vibrational redistribution* to optically dark modes—this is the faster process, which determines the timescale observed; and *dissipation to the environment*, i.e. neighbouring sites on the same or adjacent polymer chains—this process is probably one to two orders of magnitude slower. Photomodulation [18] and photocurrent [15] action spectra have been interpreted in terms of thermally activated singlet dissociation, with the on-site vibrational energy (both visible and dark) considered as thermal energy—in this context the term 'hot exciton' has been coined.

In addition to the vibrational energy, higher excited electronic states have to be considered as possible intermediates to charge separation. Advanced quantum chemical calculations [23] show that there are higher-lying neutral states with a large separation between positive and negative charge distribution centres, which are more likely to dissociate. In figure 8 we compare transient transmission spectra of *m*-LPPP for excitation energies of 3.2 and 4.8 eV. The spectra are normalized at the PB peak, to show the relative intensities of the singlet and polaron spectral features. It is evident that the higher-energy pump photons generate more charges. This can be rationalized with the assumption that charge separation takes place from higher-lying singlet states S_m.

High singlets can be reached following two possible pathways, besides direct population:

(i) *The sequential process* suggests that two pump photons are absorbed sequentially during excitation, in a step-like transition with S_1 as the intermediate, leading to population of

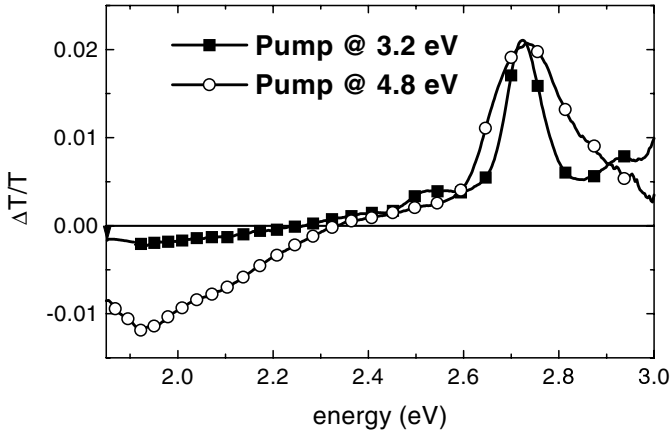

Figure 8. Transient transmission spectra of *m*-LPPP films at room temperature obtained by excitation at 3.2 eV (solid squares) and 4.8 eV (empty circles). After normalization at the bleaching peak, the larger polaron population is evident for the higher pump photon energy. Note also a spectral broadening in the latter spectrum, due to a larger distribution of excited sites.

S_n [24]. This is supported by the increasing CPG efficiency with increasing pump intensity in PFO.

(ii) *The singlet–singlet annihilation* process, based on excited state energy transfer, $S_1 + S_1 \rightarrow S_n + S_0$. This is distinct from the previous one because it is efficient when the S_1 density is high enough, typically during a few picoseconds following the photoexcitation, while the sequential mechanism is active only over the duration of the pump pulse (typically $<$200 fs).

Charge generation from higher-lying states can be directly tested by re-exciting the singlet state (S_1) with a second pump pulse (called the 'push' in the following), and probing the resulting charge carriers. One possible probe is provided by the PC in excitation cross-correlation experiments. In such a technique a first pump pulse generates singlet states ($S_0 \rightarrow S_1$) within the active layer of an organic photodiode. These S_1 states are re-excited to a higher-lying state by a second time-delayed pulse exactly resonant with a transition ($S_1 \rightarrow S_n$). (Note that the S_n discussed here, depending on the energy of the second pulse, can be different from the one reached via the above-described processes, since there is usually more than one transition $S_1 \rightarrow S_n$ with a high transition matrix element.) Dissociation is monitored via the transient change of the PC response in single-layer devices.

In a series of such experiments on *m*-LPPP diodes, PC increase consistent with S_n-mediated charge generation has been observed [25]. In figure 9 the PC enhancement ΔPC_{cc} as a function of the pump–push delay τ_r is compared with the differential transmission $\Delta T/T$ at the spectral position of the push pulse. If the charge quantum yield from the push were independent of τ_r, the number of charges generated via re-excitation would be proportional to the number of S_1 states and the two types of dynamics would be exactly the same. The faster dynamics of ΔPC_{cc} indicates that the charge quantum yield decreases rapidly with increasing τ_r—yielding a measure of the time dependence of the S_n dissociation probability $p_n(\tau_r)$. Although a strict proportionality cannot be inferred, it is intuitive to conjecture that $p_n(\tau_r)$ can be correlated with $p_1(t)$ for $t = \tau_r$, the dissociation probability of the S_1 state at the moment of its re-excitation. The function $p_1(t) = p_1(i(t), E_{vib}(t))$ is a convolution of the

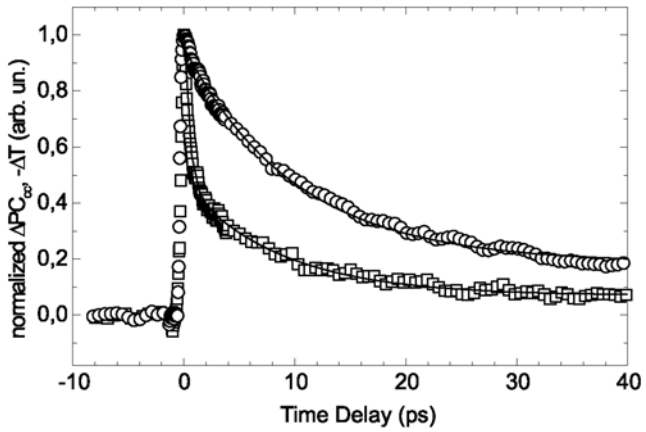

Figure 9. PC cross-correlation (open squares) compared to transient absorption of S_1 (open circles) in *m*-LPPP. Solid curves are single-exponential (upper) or bi-exponential (lower) fits (from [22]).

dependence of p_1 on the site i and the vibrational energy E_{vib}, which are both functions of time as the excitation energy migrates between sites and the vibrational energy is dissipated. A detailed discussion of the interplay between migration and vibrational relaxation is given in [26], which treats similar double-excitation measurements, but with optical monitoring of the induced excited state dynamics via transient absorption.

5. Triplet excitons

Competing with radiative decay, a number of non-radiative processes, which are common to most organic molecules in the solid state, can efficiently deactivate the lowest excited state. Internal conversion is the process of energy transfer, S_1–S_0^*, in which the electronic energy in S_1 is transformed into vibrational energy of S_0 (indicated by the asterisk). To the first approximation, empirical laws worked out for linear conjugated molecules, such as polyenes, are also valid for CP—such as the gap law [27]. The latter is based on the harmonic approximation, and it may fail for higher-lying excited state transitions (e.g. S_n–S_1) due to anharmonicity of the nuclear potential energy [22]. The chain environment can act as an energy bath of accepting vibrational modes or as modulator of the DOS. For instance in ring containing conjugated chains, torsional modes are coupled specifically with the solvent cage, leading to dramatic variation in the IC rate upon changing the solvent [28].

Intersystem crossing (ISC) to the triplet manifold can be important in systems which contain heavy atoms, where the spin-flip rate can be high. We recall that a spin flip, induced by the spin–orbit coupling operator, is characterized by a triplet population build-up matching the singlet decay kinetics, since its rate is directly proportional to the number of singlets. This allows it to be clearly distinguished from two other mechanisms generating triplets: the radical pair recombination and the singlet fission mechanisms. The former, also proposed in the photophysics of some biological molecular aggregates [29], has been invoked to explain ultrafast triplet generation in *para*-hexaphenyl (PHP) polycrystalline films [30]. Basically it is the same event as is taking place in LEDs, where oppositely charged particles coalesce into a neutral state (either triplet or singlet). While the physics of this interaction is still an area of investigation, some results seem complete [31]. For oligomers the probability of forming a triplet is 75%—that is, 25% for the singlet, which is consistent with the statistical limit. In

long chains this branching ratio may be higher or lower. An electric field-assisted pump–probe combination in a biased LED provides a tool for directly monitoring charge recombination dynamics in both time and frequency domains, because the pump pulse provides a trigger ($t = 0$) to start the observation of the charge recombination. According to the radical pair model, ultrafast photoinduced triplet generation needs the initial hot state to be separated into charges, which subsequently recombine. This model is backed by electric field-assisted pump–probe experiments on PHP nanocrystalline films, clearly showing enhanced triplet generation under an electric field (and with no electrical current) [30].

Fission is the separation of a singlet state into a pair of triplet states, yet with overall singlet multiplicity (for the $\Delta S = 0$ selection rule to be respected). The process may occur from a high-lying singlet during thermalization or from S_1. In this case the overall yield of triplets is very high, even up to unity, making the phenomenon much more evident. This is the case for poly-diacetylene (PDA), whose lowest singlet S_1 is believed to be of covalent character [32], i.e. a spin-wave excitation, which is unstable against decay into triplet pairs. Note that ISC by spin flips is inconsistent with unitary efficiency on the picosecond timescale. Ultrafast build-up of the triplet population has been measured in PDA chains in solution, following excitation with optical pulses less than 10 fs in duration, yielding a time constant of 70 fs, which is consistent with diffusion of triplet states along the conjugated backbone [33]. Energy conservation selects those singlet states, among the covalent manifold, that can undergo fission, according to $E_S \geqslant 2E_T$. The fissioning states may be populated by direct transition, following relaxation from above, or indirectly by bimolecular processes such as $S_1 + S_1 \rightarrow S_n + S_0$, with the result that triplet generation appears to be hyper-linear with excitation density. This was observed in PHP, and it is known to occur in several aromatic molecular solids [34]. Singlet fission is a fundamental event in CP photophysics, which funnels energy into the triplet manifold, competing with radiative decay. Consequently the energy location of the fissioning singlet state is a parameter controlling the efficiency of PL and also EL, where it can be important if the energy of a pair of charged states exceeds that of a triplet pair.

6. Energy and charge transfer processes

Active materials in organic light-emitting diodes are sought with emission in the blue because of the need for a colour display and because blue emission can be converted to longer wavelengths. A simple, external colour conversion technique employs covering the blue-emitting OLED with a suitable dye layer, which absorbs the blue electroluminescence (EL) and has a red-shifted photoluminescence (PL) [35]. Alternatively, a more efficient internal colour conversion technique exploits energy transfer, achieved by doping the blue-light-emitting host layer with a guest acceptor emitting at lower energy. This scheme has been successfully applied both to polymer–dye and to polymer–polymer blends [36]. For instance, blue-emitting *m*-LPPP [37] was blended with red-emitting poly(perylene-co-diethynylbenzene) (PPDB) chains [38]. Due to the relative energetic positions of the highest occupied and lowest unoccupied states in these materials, energy transfer from *m*-LPPP to PPDB occurs very efficiently, so even for modest PPDB concentrations (below 1%) both the PL and EL of the blends are dominated by the red PPDB emission [39]. In addition, for blends with a very low (0.05%) PPDB concentration, efficient white-light-emitting LEDs have been demonstrated [40]. TA measurements allow the determining of the timescale and the kinetics of the energy transfer, provided a complete knowledge of both the donor and the acceptor excited state dynamics is available. The main features of TA spectra in PPDB, following excitation at 3.2 eV, are photobleaching (PB) of the HOMO–LUMO transition (peaked at 2.18 and at 2.36 eV) and PA due to transitions from the excited state to higher-lying states. The ultrafast dynamics of *m*-LPPP/PPDB blends is

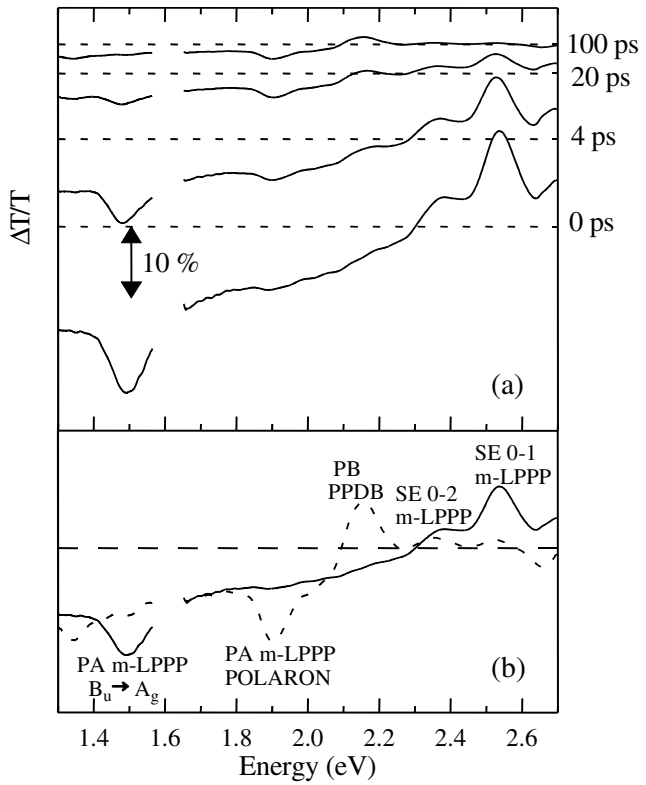

Figure 10. (a) $\Delta T/T$ spectra of a 2% *m*-LPPP/PPDB blend for various pump–probe delays. (b) Comparison for 0 ps (solid) and 100 ps (dashed, multiplied by 10) pump–probe delays (from [40]).

depicted in figure 10, reporting TA spectra of the 2% PPDB concentration blend for different pump–probe delays. For $\tau_D = 0$ ps the differential spectrum closely resembles that of pure *m*-LPPP (figure 2), indicating that this is the only excited chromophore because of the low PPDB concentrations. Following the time evolution of the $\Delta T/T$ spectrum, we observe a decay of *m*-LPPP features, with essentially no SE left at 100 ps delay, and the growing of different features on the timescale of 40 ps, clearly observable in the TA spectrum at $\tau_D = 100$ ps (see figure 10(b)). The new band at 2.15 eV, as well as its weak vibronic replica at 2.36 eV, corresponds to PB of the PPDB chains. The broad PA band observed at $\tau_D = 100$ ps for probe energies lower than 2 eV can be assigned to excited state absorption in PPDB; superimposed on this band is the sharper *m*-LPPP polaron peak. *We interpret the rise of this band as due to the excitation energy transfer fromm-LPPP to PPDB*. Note that the presence of charged states on *m*-LPPP indicates their generation to be concluded much earlier than energy transfer to PPDB. The transfer dynamics becomes considerably faster for the higher concentration (figure 11) and is clearly non-exponential. The experimental data can be modelled using the Förster theory for long-range dipole–dipole interaction, predicting a non-Markovian transfer

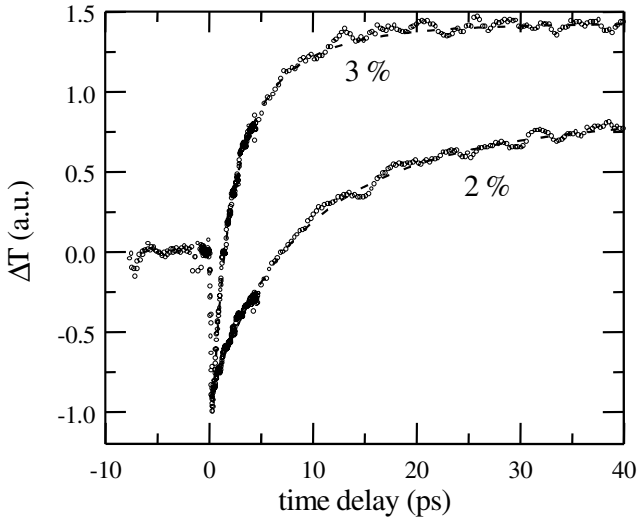

Figure 11. $\Delta T/T$ traces for 2% and 3% PPDB concentrations (open circles) and fits (dashed curves) (from [40]).

rate, according to

$$\frac{\mathrm{d}N_D}{\mathrm{d}t} = -\gamma t^{-1/2} N_D - \frac{N_D}{\tau}$$
$$\frac{\mathrm{d}N_A}{\mathrm{d}t} = +\gamma t^{-1/2} N_D \tag{9}$$

where N_D and N_A are donor (m-LPPP) and acceptor (PPDB) populations, respectively.

The constant γ is proportional to the density of the acceptors and to the overlap integral between the donor emission and the acceptor absorption spectra. Fits of the data according to the model provide values of the γ-parameter of 0.72×10^{-6} s$^{-1/2}$ and 1.03×10^{-6} s$^{-1/2}$ for the 2 and 3% blends, respectively.

Transient spectroscopy can also be used for studying ultrafast charge separation in donor–acceptor systems, envisaged for photovoltaic conversion. This is an early step in the device performance, and should be known in great detail to allow further optimization of the photovoltaic energy conversion using polymers in the active layer of plastic solar cells [41, 42]. Time-resolved spectroscopy has revealed that photoexcitation of a solid-state blend, consisting of a poly(p-phenylene vinylene) (PPV) as a donor and a methanofullerene derivative as an acceptor, results in an ultrafast forward photoinduced electron transfer reaction at the polymer/fullerene interface [43–45]. The experiments were based on observation of the temporal evolution of spectroscopical features assigned to PPV cations and fullerene anions (PA in the visible and near-IR respectively), unequivocal fingerprints for the electron transfer reaction. In particular, the initial PPV SE was observed to quickly decay into PA (due to positive polarons) when fullerene was added to the polymer, thus determining the electron transfer timescale. A time constant of 45 fs was determined for the process, assuming exponential kinetics. In general, the recombination of charges is much slower and extends into the millisecond time domain due to intermolecular charge migration and localization of charges on different sites in the film [46]. By linking organic donors to fullerenes via a covalent bond, intramolecular photoinduced charge separation [47–50] can be investigated, as a step toward chemical engineering of the process. Such phenomena were studied within two

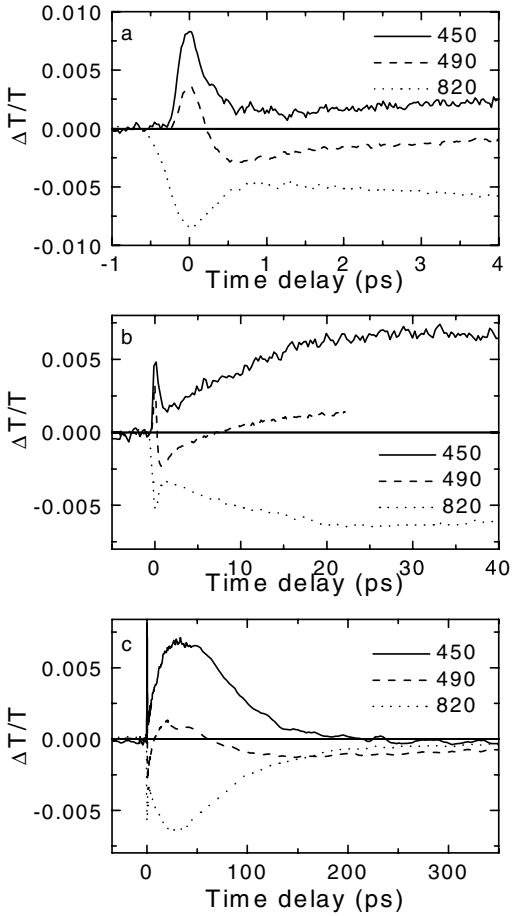

Figure 12. TA traces for OPV4-C_{60} in the polar solvent *o*-dichlorobenzene ($\varepsilon = 9.93$) at different timescales for the wavelengths indicated (from [48]): 450 nm (PB of OPV4), 490 nm (SE of OPV4) and 820 nm (PA of OPV4).

oligo(*p*-phenylene vinylene)-fulleropyrrolidine dyads with three and four phenyl rings (OPV3-C_{60} and OPV4-C_{60}) with femtosecond pump–probe spectroscopy in solvents of different polarity [51, 52]. Femtosecond differential transmission dynamics experiments have shown that after photoexcitation of the linear chain in OPV4-C_{60} in solution, the initial OPV4(S_1) state is deactivated by an efficient intramolecular singlet energy transfer to the fullerene moiety with a time constant of about 200 fs, irrespective of the polarity of the solvent. In a polar solvent, however, this subpicosecond singlet energy transfer is followed by charge separation within the OPV4-C_{60} dyad with a time constant of 13 ps. The lifetime of the intramolecular charge-separated state, created via the two-step mechanism, is 50 ps. Figure 12 contains a complete picture of the photophysical dynamics in OPV4-C_{60} in the polar solvent *o*-dichlorobenzene ($\varepsilon = 9.93$) following optical excitation with 200 fs pulses at 3.2 eV. The initial TA dynamics at 450 nm (PB of OPV4), 490 nm (SE of OPV4) and 820 nm (PA of OPV4) show energy transfer within the dyad. A new absorption band centred at 820 nm starts to grow approximately 1 ps after the excitation pulse, subsequent to the ultrafast deactivation of the OPV4(S_1) state. This PA signal is attributed to the high-energy ($D_2 \leftarrow D_0$) absorption of the (doublet) OPV4 radical cation. OPV4 ground state bleaching at 450 nm reappears, confirming that the newly

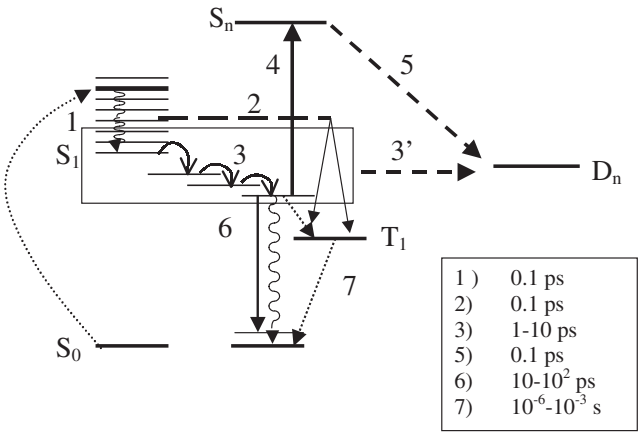

Figure 13. An overall diagram of the photophysical processes following photoexcitation (curved dotted arrow) to a vibronic level of S_1 in CPs. 1 = intrachain vibrational relaxation; 2 = singlet fission into triplet pair; 3 = interchain relaxation (spectral migration); 3 = singlet dissociation into charged states; 4 = population of S_n; 5 = S_n dissociation; 6 = deactivation of relaxed S_1, comprising radiative decay, internal conversion and intersystem crossing; 7 = deactivation of the triplet state, mainly radiationless.

formed excited state is related to the OPV4 moiety. At 490 nm, the initial OPV4 ground state bleaching/SE changes sign rapidly, upon energy transfer, to become MP-C_{60} $S_n \leftarrow S_1$ absorption and then changes sign again as the charge transfer occurs and the OPV4 ground state bleaching reoccurs. These signals show identical temporal evolutions. They start to grow 1 ps after the excitation pulse with a time constant of 13 ps, reach a maximum after 30 ps and subsequently decay with a time constant of 50 ps in ≈200 ps.

7. Conclusions

Several examples of time-resolved experiments, mainly related to *m*-LPPP, a prototypical model system for CP, have been reported. The emerging photophysical scenario contains a wealth of phenomena, some not yet fully understood, surely correlated to molecular physics but with a distinctive character. The tentative summary is drawn in figure 12, which includes the relaxation paths and their relative timescale. CPs stay in between inorganic semiconductors and organic molecules, with peculiar characteristics which make them unique for applications. Coupling of the electronic transitions to intrachain phonons, with energy in the 10^3 wavenumber range, and the very large number of nuclear degrees of freedom are responsible for the scaling down of the typical response time to the electromagnetic perturbation. Several processes are taking place within 1 ps after photoexcitation, justifying the extended use of subpicosecond probes. The recent availability of reliable devices, with repeatable and standard performances, opens up a new possibility for investigating the fundamental physics of these materials. The success of CP application, now leading to marketable products, is the outcome of the early basic research. The technological potential now presents a challenge as regards achieving a more basic understanding.

Acknowledgments

The authors want to express their gratitude to all the colleagues who contributed to the work cited in this article, in particular to G Cerullo and W Graupner for skilful help in the laboratory and numerous discussions, both face to face and intercontinentally via electronic media. CG is deeply indebted to the group of S De Silvestri for the pleasant, both scientifically and socially stimulating environment, provided by them during his long-term stay in the course of the TMR-EUROLED project.

References

[1] Schön J H, Kloc Ch, Dodabalapur A and Batlogg B 2000 *Science* **289** 599
[2] Heeger A J, Kivelson S, Schrieffer J R and Su W P 1988 *Rev. Mod. Phys.* **60** 781
[3] Kersting R, Lemmer U, Marth R F, Leo K, Kurz H, Bässler H and Göbel E O 1993 *Phys. Rev. Lett.* **70** 3820
[4] Alfano R R and Shapiro S L 1970 *Phys. Rev. Lett.* **24** 584
[5] Rulliere C (ed) 1998 *Femtosecond Laser Pulses* (Berlin: Springer)
[6] Nisoli M *et al* 1994 *Opt. Lett.* **19** 1973
Wilson K R and Yakovlev V 1997 *J. Opt. Soc. Am.* B **14** 444
[7] Stampfl J, Tasch S, Scherf U and Leising G 1995 *Synth. Met.* **71** 2125
[8] Tasch S, Niko A, Leising G and Scherf U 1996 *Appl. Phys. Lett.* **68** 1090
[9] Stagira S, Zavelani-Rossi M, Nisoli M, De Silvestri S, Lanzani G G, Zenz C, Mataloni P and Leising G 1998 *Appl. Phys. Lett.* **73** 2860
[10] Lemmer U, Haugeneder A, Kallinger C and Feldmann J 2000 *Semiconducting Polymers* ed G Hadziioannou and P F van Hutten (Weinheim: Wiley–VCH) p 309
[11] Graupner W, Lanzani G, Leising G, Nisoli M, De Silvestri S and Scherf U 1996 *Phys. Rev. Lett.* **76** 847
[12] Harrison N T, Hayes G R and Phillips R T 1996 *Phys. Rev. Lett.* **77** 1881
[13] Denton G J, Tessler N, Harrison N T and Friend R H 1997 *Phys. Rev. Lett.* **78** 733
[14] Maniloff E S, Klimov V I and McBranch D W 1997 *Phys. Rev.* B **56** 1876
[15] Dexheimer S L, Vareka W A, Mittleman D, Zettl A and Shank C V 1995 *Chem. Phys. Lett.* **235** 552
[16] Cerullo G, Stagira S, Nisoli M, De Silvestri S, Lanzani G, Kranzelbinder G, Graupner W and Leising G 1998 *Phys. Rev.* B **57** 12 806
[17] Stagira S, Nisoli M, Lanzani G, De Silvestri S, Cassano T, Tommasini R, Babudri F, Farinola G M and Naso F 2001 *Phys. Rev.* B **64** 205205
[18] Kersting R, Lemmer U, Deussen M, Bakker H J, Mahrt R F, Kurz H, Arkhipov V I, Bässler H and Göbel E O 1994 *Phys. Rev. Lett.* **73** 1440
[19] Arkhipov V I, Emilianova E V and Bässler H 1999 *Phys. Rev. Lett.* **82** 1321
[20] Graupner W, Cerullo G, Lanzani G, Nisoli M, List E J W, Leising G and De Silvestri S 1998 *Phys. Rev. Lett.* **81** 3259
[21] Vissenberg M C J M and de Jong M J M 1998 *Phys. Rev.* B **57** 2667
[22] Wohlgenannt M, Graupner W, Leising G and Vardeny Z V 1999 *Phys. Rev. Lett.* **82** 3344
[23] Köhler A, dos Santos D A, Beljonne D, Shuai Z, Brédas J L, Holmes A B, Kraus A, Müllen K and Friend R H 1998 *Nature* **392** 903
[24] Silva C, Dhoot A S, Russel D M, Stevens M A, Arias A C, MacKenzie J D, Greenham N C and Friend R H 2001 *Phys. Rev.* B **64** 125211
[25] Zenz C, Lanzani G, Cerullo G, Graupner W, Leising G and De Silvestri S 2001 *Chem. Phys. Lett.* **341** 63
[26] Gadermaier C *et al* 2002 *Phys. Rev. Lett.* **89** 117402
[27] Englman R and Jortner J 1970 *J. Mol. Phys.* **18** 145
[28] Lanzani G, Cerullo G, De Silvestri S, Barbarella G and Sotgiu G 2001 *J. Chem. Phys.* **115** 1623
[29] Gradinaru C C *et al* 2001 *Proc. Natl Acad. Sci. USA* **98** 2364
[30] Zenz C, Cerullo G, Lanzani G, Graupner W, Meghdadi F, Leising G and De Silvestri S 1999 *Phys. Rev.* B **59** 14 336
[31] Cao Y *et al* 1999 *Nature* **397** 414
Wohlgenannt M *et al* 2001 *Nature* **409** 494
Shuai Z *et al* 2000 *Phys. Rev. Lett.* **84** 131
[32] Tavan P and Schulten K 1987 *Phys. Rev.* B **36** 4337

[33] Lanzani G, Cerullo G, Zavelani-Rossi M, De Silvestri S, Comoretto D, Musso G and Dellepiane G 2001 *Phys. Rev. Lett.* **87** 187402
[34] Pope M and Swenberg C E 1999 *Electronic Processes in Organic Crystals and Polymers* (New York: Oxford University Press)
[35] Tasch S, Brandstätter C, Meghdadi F, Leising G, Athouel L and Froyer G 1997 *Adv. Mater.* **9** 33
[36] Hu B, Yang Z and Karasz F E 1994 *J. Appl. Phys.* **76** 2419
Haring Bolivar P, Wegmann G, Kersting R, Deussen M, Lemmer U, Mahrt R F, Bässler H, Göbel E O and Kurz H 1995 *Chem. Phys. Lett.* **245** 534
Lee J, Kang I, Hwang D, Shim H, Jeoung S and Kim D 1996 *Chem. Mater.* **8** 1925
Berggren M, Dodabalapur A, Slusher R E and Bao Z 1997 *Nature* **389** 466
Cerullo G, Stagira S, Zavelani-Rossi M, De Silvestri S, Virgili T, Lidzey D G and Bradley D D C 2001 *Chem. Phys. Lett.* **335** 27
[37] Scherf U and Müllen K 1992 *Polymer* **33** 2443
[38] Quante H, Schlichting O, Rohr U, Geerts Y and Müllen K 1996 *Macromol. Chem. Phys.* **197** 4029
[39] Tasch S, Hochfilzer C, List E, Leising G, Quante H, Geerts Y, Scherf U and Müllen K 1997 *Phys. Rev.* B **56** 4479
[40] Tasch S, List E J W, Ekström O, Graupner W, Leising G, Schlichting P, Rohr U, Geerts Y, Scherf U and Müllen K 1997 *Appl. Phys. Lett.* **71** 2883
[41] Sariciftci N S, Smilowitz L, Heeger A J and Wudl F 1992 *Science* **258** 1474
[42] Yu G, Gao Y, Hummelen J C, Wudl F and Heeger A J 1995 *Science* **270** 1789
[43] Kraabel B, McBranch D, Sariciftci N S and Heeger A J 1994 *Phys. Rev.* B **50** 18 543
[44] Kraabel B, Hummelen J C, Vacar D, Moses D, Sariciftci N S and Heeger A J 1996 *J. Chem. Phys.* **104** 4267
[45] Brabec C J, Zerza G, Sariciftci N S, Cerullo G, De Silvestri S, Luzzati S and Hummelen J C 2002 *Chem. Phys. Lett.* at press
[46] Meskers S C J, van Hal P A, Spiering A J H, van der Meer A F G, Hummelen J C and Janssen R A J 2000 *Phys. Rev.* B **61** 9917
[47] Martín N, Sánchez L, Illescas B and Pérez I 1998 *Chem. Rev.* **98** 2527
[48] Prato M 1997 *J. Mater. Chem.* **7** 1097
[49] Imahori H and Sakata Y 1997 *Adv. Mater.* **9** 537
[50] Imahori H and Sakata Y 1999 *Eur. J. Org. Chem.* 2445
[51] van Hal P A, Janssen R A J, Lanzani G, Cerullo G, Zavelani-Rossi M and De Silvestri S 2001 *Phys. Rev.* B **64** 75 206
[52] van Hal P A, Janssen R A J, Lanzani G, Cerullo G, Zavelani-Rossi M and De Silvestri S 2001 *Chem. Phys. Lett.* **345** 33